

Comparative study of correlation effects in  $\text{CaVO}_3$  and  $\text{SrVO}_3$ I. A. Nekrasov,<sup>1,2</sup> G. Keller,<sup>2</sup> D. E. Kondakov,<sup>1,2,3</sup> A. V. Kozhevnikov,<sup>1,2,3</sup> Th. Pruschke,<sup>2</sup> K. Held,<sup>4</sup> D. Vollhardt,<sup>2</sup> and V. I. Anisimov<sup>1,2</sup><sup>1</sup>*Institute of Metal Physics, Russian Academy of Sciences-Ural Division, 620219 Yekaterinburg GSP-170, Russia*<sup>2</sup>*Theoretical Physics III, Center for Electronic Correlations and Magnetism, University of Augsburg, 86135 Augsburg, Germany*<sup>3</sup>*Department of Theoretical Physics and Applied Mathematics, USTU, 620002 Yekaterinburg Mira 19, Russia*<sup>4</sup>*Max Planck Institute for Solid State Research, Heisenbergstrasse 1, 70569 Stuttgart, Germany*

(Received 20 January 2005; revised manuscript received 3 June 2005; published 7 October 2005)

We present parameter-free LDA+DMFT (local density approximation+dynamical mean field theory) results for the many-body spectra of cubic  $\text{SrVO}_3$  and orthorhombic  $\text{CaVO}_3$ . Both systems are found to be strongly correlated metals, but not on the verge of a metal-insulator transition. In spite of the considerably smaller V—O—V bonding angle in  $\text{CaVO}_3$ , the LDA+DMFT photoemission spectra of the two systems are very similar, their quasiparticle parts being almost identical. The calculated x-ray absorption spectra show more pronounced, albeit still small, differences. This is in contrast to earlier theoretical and experimental conclusions, but in agreement with recent bulk-sensitive photoemission and x-ray absorption experiments.

DOI: [10.1103/PhysRevB.72.155106](https://doi.org/10.1103/PhysRevB.72.155106)

PACS number(s): 71.27.+a, 71.30.+h

## I. INTRODUCTION

Transition metal oxides are an ideal laboratory for the study of electronic correlations in solids. In these materials, the  $3d$  bands are comparatively narrow with width  $W \approx 2-3$  eV so that electronic correlations, induced by the local Coulomb interaction  $\bar{U} \approx 3-5$  eV, are strong. For  $\bar{U}/W \ll 1$ , we have a weakly correlated metal and the local density approximation (LDA) (see Ref. 1 for a review) works. In the opposite limit  $\bar{U}/W \gg 1$  and for an integer number of  $3d$  electrons, we have a Mott insulator with two splitted Hubbard bands as described by Hubbard's I and III approximations<sup>2</sup> or the LDA+U method.<sup>3</sup> Transition metals are, however, in the “in-between” regime,  $\bar{U}/W = \mathcal{O}(1)$ , where the metallic phase is strongly correlated with coexisting *quasiparticle* peak at the Fermi level and Hubbard side bands.

Dynamical mean-field theory (DMFT),<sup>4-7</sup> a modern, non-perturbative many-body approach, is able to capture the physics in the whole range of parameters from  $\bar{U}/W \ll 1$  to  $\bar{U}/W \gg 1$  for model Hamiltonians, like the one-band Hubbard model (for an introduction into DMFT and its applications, see Ref. 8). And, with the recent merger<sup>9-11</sup> of LDA and DMFT, we are now able to handle this kind of correlation physics within realistic calculations for transition metal oxides.

A particularly simple transition metal oxide system is  $\text{Ca}_{1-x}\text{Sr}_x\text{VO}_3$  with a  $3d^1$  electronic configuration and a cubic perovskite lattice structure. The latter is ideal for  $\text{SrVO}_3$  and orthorhombically distorted upon increasing the Ca-doping  $x$ . Fujimori *et al.*<sup>12</sup> initiated the present interest in this  $3d^1$  series, reporting a pronounced lower Hubbard band in the photoemission spectra (PES) which cannot be explained by conventional LDA. Subsequently, thermodynamic properties were studied, and the Sommerfeld coefficient, resistivity, and paramagnetic susceptibility were found to be essentially independent of  $x$ .<sup>13</sup>

On the other hand, PES and bremsstrahlungs isochromat spectra (BIS)<sup>14</sup> seemed to imply dramatic differences between  $\text{CaVO}_3$  and  $\text{SrVO}_3$ , with  $\text{CaVO}_3$  having (almost) no spectral weight at the Fermi energy. Rozenberg *et al.*<sup>15</sup> interpreted these results in terms of the (DMFT) Mott-Hubbard transition in the half-filled single-band Hubbard model. With the same theoretical ansatz, albeit different parameters, the optical conductivity<sup>16</sup> and the PES experiments<sup>17</sup> for different dopings  $x$  were reproduced.

The puzzling discrepancy between these spectroscopic and the thermodynamic measurements, suggesting a Mott-Hubbard metal-insulator transition or not, were resolved recently by bulk-sensitive PES obtained by Maiti *et al.*<sup>17</sup> and Sekiyama *et al.*<sup>18,19</sup> In the latter work it was shown that (i) the technique of preparing the sample surface (which should preferably be done by fracturing) is very important, and that (ii) the energy of the x-ray beam should be large enough to increase the photoelectron escape depth to achieve bulk sensitivity. Theoretically, pronounced differences between  $\text{SrVO}_3$  surface and bulk spectra were reported by Liebsch.<sup>20</sup> Besides bulk sensitivity, the beam should provide a high instrumental resolution (about 100 meV in Refs. 18 and 19). With these experimental improvements, the PES of  $\text{SrVO}_3$  and  $\text{CaVO}_3$  were found to be almost identical,<sup>17-19</sup> implying consistency of spectroscopic and thermodynamic results at last. This is also in accord with earlier  $1s$  x-ray absorption spectra (XAS) by Inoue *et al.*,<sup>21</sup> which differ only slightly above the Fermi energy, but in contrast to the BIS data.<sup>14</sup> Sekiyama *et al.*<sup>19</sup> also compared their high-resolution bulk-sensitive PES with parameter-free LDA+DMFT calculations, reporting good agreement.

Originally, we presented these LDA+DMFT calculations in a preprint<sup>22</sup> which was, however, superceded by a joint experimental and theoretical letter,<sup>19</sup> making the present, more detailed presentation, including a comparison with XAS,<sup>21</sup> necessary. Also note that independent LDA+DMFT calculations for  $3d^1$  vanadates, including  $\text{SrVO}_3$  and  $\text{CaVO}_3$ , have meanwhile been reported by Pavarini *et al.*<sup>23,24</sup> Recently, Anisimov *et al.*, using a full-orbital computational

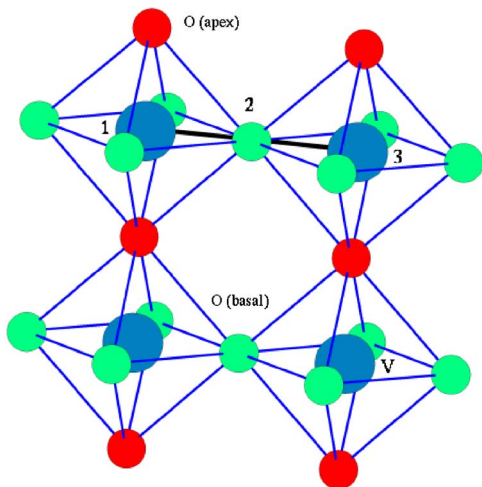


FIG. 1. (Color online)  $\text{SrVO}_3$ , an ideal cubic perovskite, with  $\text{V—O—V}$  angle  $\theta = \angle 123 = 180^\circ$ ; V: large ions,  $\text{O}_{\text{basal}}$ : small bright ions, and  $\text{O}_{\text{apex}}$ : small dark ions.

scheme based on a Wannier functions formalism for LDA+DMFT, presented total densities of states (DOS) for  $\text{SrVO}_3$  in good agreement with PES.<sup>25</sup> A LDA+DMFT scheme with a few-orbital NMTD downfolded LDA Hamiltonian<sup>26</sup> was implemented by Nekrasov *et al.* to obtain  $\mathbf{k}$ -resolved spectral functions of  $\text{SrVO}_3$ .<sup>27</sup>

We start with discussing the structural differences between  $\text{SrVO}_3$  and  $\text{CaVO}_3$  in Sec. II A, based on the most recent crystallographic data provided by Inoue.<sup>28</sup> How these differences reflect in the LDA results is shown in Sec. II B, before we turn to the LDA+DMFT scheme in Sec. III A and the effects of electronic correlations in Sec. III B. Section IV concludes our presentation.

## II. $\text{SrVO}_3$ VS. $\text{CaVO}_3$ : STRUCTURAL DIFFERENCES AND LDA RESULTS

### A. Structural differences

Both  $\text{SrVO}_3$  and  $\text{CaVO}_3$  are perovskites, with  $\text{SrVO}_3$  in the ideal cubic structure  $Pm\bar{3}m$ <sup>29</sup> (Fig. 1) and  $\text{CaVO}_3$  in the orthorhombically distorted ( $\text{GdFeO}_3$ )  $Pbnm$  structure<sup>28,30</sup> (Fig. 2). The ideal cubic structure of  $\text{SrVO}_3$  implies that the  $\text{VO}_6$  octahedra, the main structural elements of the crystal, are not distorted: The  $\text{V—O}_{\text{basal}}$  and  $\text{V—O}_{\text{apex}}$  distances are the same, the  $\text{O}_{\text{apex}}\text{—V—O}_{\text{basal}}$  and  $\text{O}_{\text{basal}}\text{—V—O}_{\text{basal}}$  angles are  $90^\circ$ , and the  $\text{V—O—V}$  bond angles are exactly  $180^\circ$ . The substitution of the large  $\text{Sr}^{2+}$  ions by smaller  $\text{Ca}^{2+}$  ions leads to a tilting, rotation, and distortion of the  $\text{VO}_6$  octahedra. Nonetheless, in  $\text{CaVO}_3$ , both the  $\text{V—O}_{\text{basal}}$  and the  $\text{V—O}_{\text{apex}}$  distances are practically the same. Therefore, the most important feature of the distortion is the change of the  $\text{V—O}_{\text{basal}}\text{—V}$  and  $\text{V—O}_{\text{apex}}\text{—V}$  angles, which determines the strength of the effective  $\text{V-3d-V-3d}$  hybridization and, hence, the bandwidth. Due to the rotation and tilting of the octahedra both angles (one of them is marked as  $\angle 123$  in Figs. 1 and 2) have the same value  $\theta = 180^\circ$  for  $\text{SrVO}_3$  and  $\theta_{\text{basal}} \approx 161^\circ$ ,  $\theta_{\text{plane}} \approx 163^\circ$  for  $\text{CaVO}_3$ .

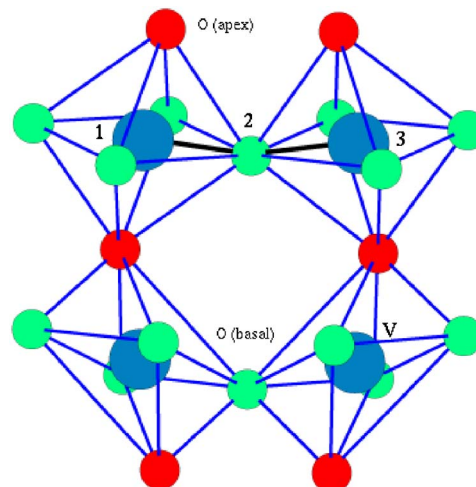


FIG. 2. (Color online)  $\text{CaVO}_3$ , an orthorhombically distorted perovskite, with  $\text{V—O—V}$  angles  $\theta_{\text{basal}} \approx 161^\circ$ ,  $\theta_{\text{plane}} \approx 163^\circ$ ; V: large ions,  $\text{O}_{\text{basal}}$ : small bright ions, and  $\text{O}_{\text{apex}}$ : small dark ions. The local  $c$  axis, later used for the definition of the orbitals, is directed along the tilted  $\text{V—O}_{\text{apex}}$  direction.

### B. LDA results

The valence states of  $\text{SrVO}_3$  and  $\text{CaVO}_3$  consist of completely occupied oxygen  $2p$  bands and partially occupied  $\text{V-3d}$  bands. Since the V ion has a formal oxidation of  $4+$ , there is one electron per V ion occupying the  $d$  states (configuration  $d^1$ ). In Figs. 3 and 4 the LDA DOS are presented for both compounds, as calculated by the linearized muffin-tin orbital method (LMTO)<sup>31</sup> with an orthogonal basis set of  $\text{Sr}(5s, 5p, 4d, 4f)$ ,  $\text{Ca}(4s, 4p, 3d)$ ,  $\text{V}(4s, 4p, 3d)$ , and  $\text{O}(3s, 2p, 3d)$  orbitals.<sup>32</sup> These results are in agreement with previous LDA calculations in the basis of augmented plane waves (APW) by Tagekahara.<sup>33</sup> For a combination of the LDA band structure with many-body techniques,<sup>9</sup> however, the atomic-like LMTO wave functions employed here are

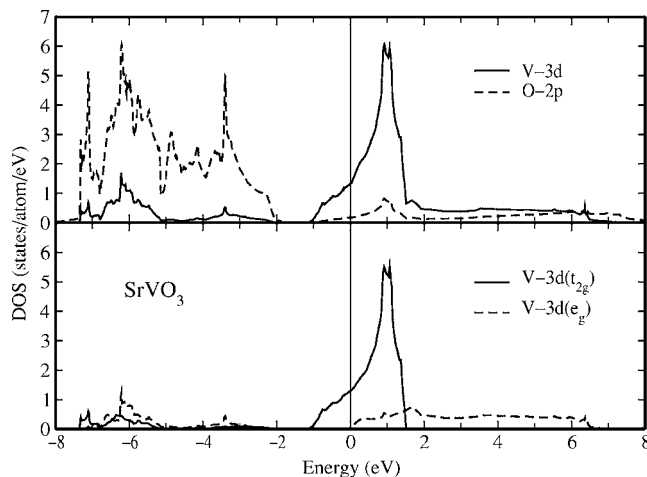


FIG. 3. DOS of  $\text{SrVO}_3$  as calculated by LDA(LMTO). Upper panel:  $\text{V-3d}$  (full line) and  $\text{O-2p}$  (dashed line) DOS; lower panel: partial DOS of  $\text{V-3d}(e_g)$  (full line) and  $\text{V-3d}(t_{2g})$  (dashed line) orbitals. The Fermi level corresponds to 0 eV.

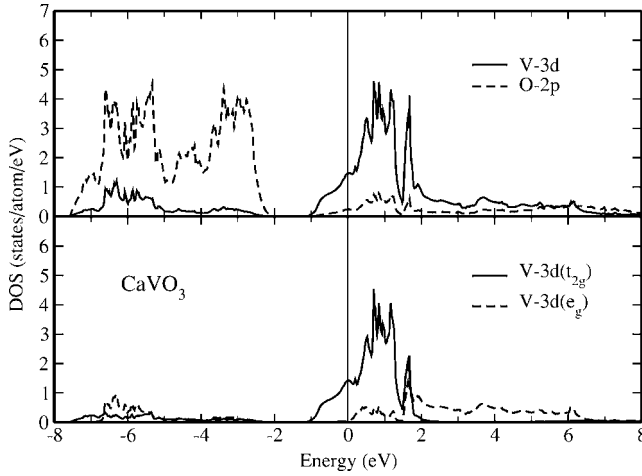


FIG. 4. DOS of  $\text{CaVO}_3$  as calculated by LDA(LMTO). Upper panel: V-3d (full line) and O-2p (dashed line) DOS; lower panel: partial DOS of V-3d( $e_g$ ) (full line) and V-3d( $t_{2g}$ ) (dashed line) orbitals. The Fermi level corresponds to 0 eV.

particularly convenient. As is apparent from Figs. 3 and 4, the O-2p states lie between  $-7.5$  and  $-2.0$  eV in  $\text{SrVO}_3$  and between  $-6.5$  and  $-1.5$  eV in  $\text{CaVO}_3$ . The 3d states of V are located between  $-1.1$  and  $6.5$  eV in  $\text{SrVO}_3$  and between  $-1.0$  and  $6.5$  eV in  $\text{CaVO}_3$ . These results are in agreement with previous LDA calculations in the basis of augmented plane waves (APW) by Tagekahara,<sup>33</sup> but for our purposes LMTO is more appropriate.

In both compounds, the V ions are in an octahedral coordination of oxygen ions. The octahedral crystal field splits the V-3d states into three  $t_{2g}$  orbitals and two  $e_g$  orbitals. In the cubic symmetry of  $\text{SrVO}_3$ , hybridization between  $t_{2g}$  and  $e_g$  states is forbidden, and the orbitals within both subbands are degenerate. In contrast, the distorted orthorhombic structure of  $\text{CaVO}_3$  allows them to mix and the degeneracy is lifted. In the lower part of Figs. 3 and 4, we present these  $t_{2g}$  and  $e_g$  subbands of the V-3d band. For both Sr and Ca compounds, the reader can see an admixture of these vanadium  $t_{2g}$  and  $e_g$  states to the oxygen 2p states in the energy region  $[-8 \text{ eV}, -2 \text{ eV}]$ . This is due to hybridization and amounts to 12% and 15% of the total  $t_{2g}$  weight for  $\text{SrVO}_3$  and  $\text{CaVO}_3$ , respectively. The main  $t_{2g}$  ( $e_g$ ) weight lies in the energy region  $[-1.1 \text{ eV}, 1.5 \text{ eV}]$  ( $[0.0 \text{ eV}, 6.5 \text{ eV}]$ ) in  $\text{SrVO}_3$  and  $[-1.0 \text{ eV}, 1.5 \text{ eV}]$  ( $[0.2 \text{ eV}, 6.5 \text{ eV}]$ ) in  $\text{CaVO}_3$ . The peak at 1.5–2 eV in the DOS of the Ca compound is formed mainly because of  $t_{2g}$ - $e_g$  hybridization. Since the energy difference between the centers of gravities of the  $t_{2g}$  and  $e_g$  subbands is comparable with the bandwidth,  $t_{2g}$  and  $e_g$  states can be considered as sufficiently separated in both compounds. Details of the  $t_{2g}$  bands for both compounds are shown in Fig. 5. The overall shape of the  $t_{2g}$  DOS is in agreement with other LDA TB-LMTO(ASA) computations.<sup>23,24</sup>

Let us now concentrate on the  $t_{2g}$  orbitals crossing the Fermi energy and compare the LDA  $t_{2g}$  DOS of  $\text{SrVO}_3$  and  $\text{CaVO}_3$ . Most importantly, the one-electron  $t_{2g}$  LDA bandwidth of  $\text{CaVO}_3$ , defined as the energy interval where the  $t_{2g}$  DOS in Fig. 5 is nonzero, is found to be only 4% smaller than that of  $\text{SrVO}_3$  ( $W_{\text{CaVO}_3} = 2.5 \text{ eV}$ ,  $W_{\text{SrVO}_3} = 2.6 \text{ eV}$ ). This

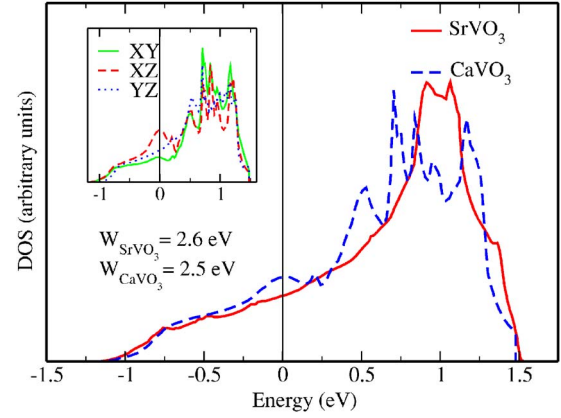


FIG. 5. (Color online) Comparison of the LDA DOS of the V-3d ( $t_{2g}$ ) band for  $\text{SrVO}_3$  (solid line) and  $\text{CaVO}_3$  (dashed line). In  $\text{CaVO}_3$  the degeneracy of the three  $t_{2g}$  bands is lifted (see inset). The bandwidth  $W_{\text{CaVO}_3} = 2.5 \text{ eV}$  is only 4% smaller than  $W_{\text{SrVO}_3} = 2.6 \text{ eV}$  (partially reproduced Fig. 2 from Ref. 19).

is in contrast to the expectation that the strong lattice distortion with a decrease of the V—O—V bond angle from  $180^\circ$  to  $162^\circ$  affects the  $t_{2g}$  bandwidth much more strongly. Such a larger effect indeed occurs in the  $e_g$  bands for which the bandwidth is reduced by 10%. Qualitatively one can understand the weak narrowing of the  $t_{2g}$  bands in terms of the effective  $t_{2g}$ - $t_{2g}$  and  $e_g$ - $e_g$  hopping parameters. The predominant contribution to the  $e_g$ - $e_g$  hopping is through a  $d$ - $p$ - $d$  hybridization, which indeed considerably decreases with increasing lattice distortion as is to be expected. This is also the case for the  $t_{2g}$  orbitals. However, for the  $t_{2g}$  orbitals, the direct  $d$ - $d$  hybridization is also important. This hybridization *increases* with increasing distortion since the  $t_{2g}$  orbital lobes then point more towards each other in the distorted structure. Altogether, the competition between (i) decreasing  $d$ - $p$ - $d$  hybridization and (ii) increasing  $d$ - $d$  hybridization results in a very small change of the  $t_{2g}$  bandwidth. This explains why previous suggestions of strongly different bandwidths are untenable. The  $dd\pi$  and  $dd\sigma$  tight-binding parameters between  $t_{2g}$  orbitals presented in the recent work by Pavarini *et al.*<sup>24</sup> for both  $\text{SrVO}_3$  and  $\text{CaVO}_3$  systems qualitatively support the arguments given above.

### III. CORRELATION EFFECTS IN $\text{SrVO}_3$ AND $\text{CaVO}_3$

#### A. Dynamical mean-field theory

As is well known, LDA does not treat the effects of strong local Coulomb correlations adequately. To overcome this drawback, we use LDA+DMFT as a nonperturbative approach to study strongly correlated systems.<sup>9–11</sup> It combines the strength of the LDA in describing weakly correlated electrons in the  $s$  and  $p$  orbitals, with the DMFT treatment of the dynamics due to local Coulomb interactions. In the present paper we will discuss the relevant parts of the LDA+DMFT approach only briefly, referring the reader to Refs. 10 and 11 for details.

The LDA+DMFT Hamiltonian can be written as

$$\hat{H} = \hat{H}_{\text{LDA}}^0 + U \sum_m \sum_i \hat{n}_{im\uparrow} \hat{n}_{im\downarrow} + \sum_{im \neq m' \sigma \sigma'} (U' - \delta_{\sigma \sigma'} J) \hat{n}_{im\sigma} \hat{n}_{im' \sigma'}. \quad (1)$$

Here, the index  $i$  enumerates the V sites,  $m$  the individual  $t_{2g}$  orbitals, and  $\sigma$  the spin.  $H_{\text{LDA}}^0$  is the one-particle Hamiltonian generated from the LDA band structure with an averaged Coulomb interaction subtracted to account for double counting;<sup>9</sup>  $U$  and  $U'$  denote the local intraorbital and inter-orbital Coulomb repulsions, and  $J$  is the exchange interaction.

We calculated these interaction strengths by means of the constrained LDA method<sup>34</sup> for SrVO<sub>3</sub>, allowing the  $e_g$  states to participate in screening.<sup>35</sup> The resulting value of the averaged Coulomb interaction is  $\bar{U}=3.55$  eV ( $\bar{U}=U'$  for  $t_{2g}$  orbitals<sup>10,36</sup>) and  $J=1.0$  eV. The intraorbital Coulomb repulsion  $U$  is then fixed by rotational invariance to  $U=U'+2J=5.55$  eV. We did not calculate  $\bar{U}$  for CaVO<sub>3</sub> because the standard procedure to calculate the Coulomb interaction parameter between two  $t_{2g}$  electrons, screened by  $e_g$  states, is not applicable for the distorted crystal structure where the  $e_g$  and  $t_{2g}$  orbitals are not separated by symmetry. On the other hand, it is well known that the change of the *local* Coulomb interaction is typically much smaller than the change in the DOS, which was found to depend only very weakly on the bond angle. That means that  $\bar{U}$  for CaVO<sub>3</sub> should be nearly the same as for SrVO<sub>3</sub>. Therefore we used  $\bar{U}=3.55$  eV and  $J=1.0$  eV for both SrVO<sub>3</sub> and CaVO<sub>3</sub>. This is also in agreement with previous calculations of vanadium systems<sup>35</sup> and experiments.<sup>16</sup>

DMFT maps the lattice problem Eq. (1) onto a self-consistent auxiliary impurity problem, which is here solved numerically by the quantum Monte Carlo (QMC) technique.<sup>37</sup> Combined with the maximum entropy method,<sup>38</sup> this technique allows us to calculate spectral functions.<sup>39–42</sup>

A computationally important simplification is due to the fact that, in ideal cubic perovskites, the (degenerate)  $t_{2g}$  states do not mix with the (degenerate)  $e_g$  states. In this particular case, the self-energy matrix  $\Sigma(z)$  is diagonal with respect to the orbital indices. Under this condition, the Green functions  $G_m(z)$  of the lattice problem can be expressed in the DMFT self-consistency equation by the Hilbert transform of the noninteracting DOS  $N_m^0(\epsilon)$ :

$$G_m(z) = \int d\epsilon \frac{N_m^0(\epsilon)}{z - \Sigma_m(z) - \epsilon}. \quad (2)$$

This procedure avoids the rather cumbersome and problematic  $\mathbf{k}$ -integration over the Brillouin zone by the analytical tetrahedron method.<sup>43</sup> Here the quantity  $N_m^0(\epsilon)$  for SrVO<sub>3</sub> and CaVO<sub>3</sub> is given by the  $t_{2g}$ -projected DOS presented in Fig. 5. We note that Eq. (2) is valid strictly only for degenerate bands. However, for CaVO<sub>3</sub> where the  $t_{2g}$  bands are slightly different (see inset of Fig. 5), Eq. (2) is still a rather good approximation since the deviation from cubic symmetry is minor. This procedure is employed as it resembles the three *effective* bands of  $t_{2g}$  character which cross the Fermi

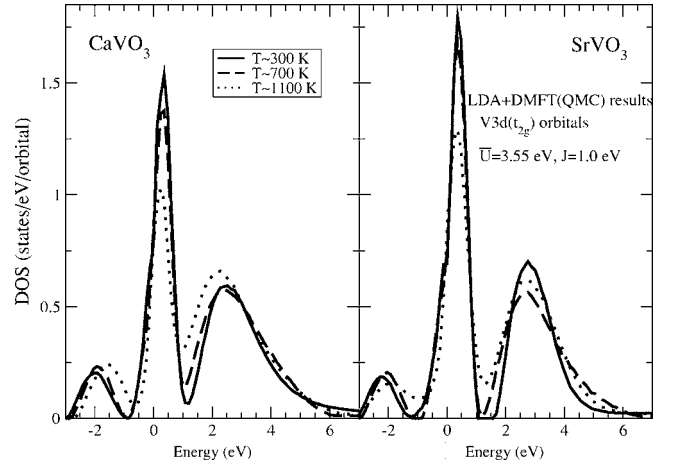


FIG. 6. LDA+DMFT(QMC) spectrum of SrVO<sub>3</sub> (right panel) and CaVO<sub>3</sub> (left panel) calculated at  $T \approx 300$  K (solid lines),  $T \approx 700$  K (dashed lines), and  $T \approx 1100$  K (dotted lines).

energy and are, hence, responsible for the low-energy physics.

## B. LDA+DMFT(QMC) results and discussion

The calculated LDA+DMFT(QMC) spectra for SrVO<sub>3</sub> (right panel) and CaVO<sub>3</sub> (left panel) are presented in Fig. 6 for different temperatures. Due to genuine correlation effects, a lower Hubbard band at about  $-1.5$  eV and an upper Hubbard band at about  $2.5$  eV is formed, with a well-pronounced quasiparticle peak at the Fermi energy. The 4% difference in the LDA bandwidth between SrVO<sub>3</sub> and CaVO<sub>3</sub> is only reflected in some additional transfer of spectral weight from the quasiparticle peak to the Hubbard bands, and minor differences in the positions of the Hubbard bands. Clearly, the two systems are not on the verge of a Mott-Hubbard metal-insulator transition. Both, SrVO<sub>3</sub> and CaVO<sub>3</sub>, are strongly correlated metals, though SrVO<sub>3</sub> is slightly less correlated than CaVO<sub>3</sub> with somewhat more quasiparticle weight, in accord with their different LDA bandwidths. As one can see from Fig. 6, the effect of temperature on the spectrum is small for  $T \lesssim 700$  K.

In the left panel of Fig. 7, we compare our LDA+DMFT spectra (300 K), which were multiplied with the Fermi function at the experimental temperature (20 K) and Gauss broadened with the experimental resolution of 0.1 eV (Ref. 18) with the experimental PES data obtained by subtracting the experimentally estimated surface and oxygen contributions. Due to the high photon energy (several hundred eV),<sup>18</sup> the PES transition matrix elements will have *no* strong energy dependence in the energy interval of a few eV studied here, which justifies that we do not take such matrix elements into account.

The quasiparticle peaks in theory and experiment are seen to be in very good agreement. In particular, their heights and widths are almost identical for both SrVO<sub>3</sub> and CaVO<sub>3</sub>. The difference in the positions of the lower Hubbard bands may be partly due to (i) the subtraction of the (estimated) oxygen contribution which might also remove some  $3d$  spectral

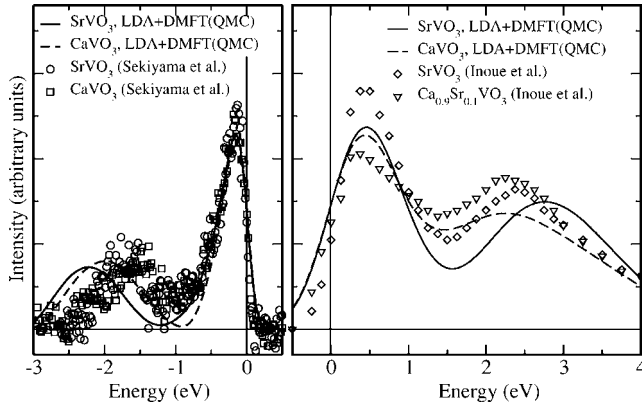


FIG. 7. Comparison of the parameter-free LDA+DMFT(QMC) spectra of SrVO<sub>3</sub> (solid line) and CaVO<sub>3</sub> (dashed line) with experiments below and above the Fermi energy. Left panel: high-resolution PES for SrVO<sub>3</sub> (circles) and CaVO<sub>3</sub> (rectangles) (Ref. 18). Right panel: 1s XAS for SrVO<sub>3</sub> (diamonds) and Ca<sub>0.9</sub>Sr<sub>0.1</sub>VO<sub>3</sub> (triangles) (Ref. 21). Horizontal line: experimental subtraction of the background intensity.

weight below  $-2$  eV, and (ii) uncertainties in the *ab initio* calculation of  $\bar{U}$ .

In the right panel of Fig. 7, we compare to the XAS data.<sup>21</sup> We consider core-hole life time effects by Lorentz broadening the spectrum with 0.2 eV,<sup>44</sup> multiply with the inverse Fermi function (80 K), and apply Gauss broadening given by the experimental resolution of 0.36 eV.<sup>28</sup> Again, the overall agreement of the weights and positions of the quasiparticle and upper  $t_{2g}$  Hubbard band is good, including the tendencies when going from SrVO<sub>3</sub> to CaVO<sub>3</sub>. For CaVO<sub>3</sub> (Ca<sub>0.9</sub>Sr<sub>0.1</sub>VO<sub>3</sub> in the experiment), the LDA+DMFT quasiparticle weight is somewhat lower than in experiment.

In contrast to one-band Hubbard model calculations, our material-specific results reproduce the strong asymmetry around the Fermi energy w.r.t. weights and bandwidths. Our results also give a different interpretation of the XAS than in Ref. 21 where the maximum at about 2.5 eV was attributed solely to the  $e_g$  band. We find that also the  $t_{2g}$  upper Hubbard band contributes in this energy range.

The slight differences in the quasiparticle peaks (see Fig. 6) lead to different effective masses, namely  $m^*/m_0=2.1$  for SrVO<sub>3</sub> and  $m^*/m_0=2.4$  for CaVO<sub>3</sub>. These theoretical values agree with  $m^*/m_0=2-3$  for SrVO<sub>3</sub> and CaVO<sub>3</sub> as obtained from de Haas-van Alphen experiments and thermodynamics.<sup>13,45</sup> We note that the effective mass of CaVO<sub>3</sub> obtained from optical experiments is somewhat larger, i.e.,  $m^*/m_0=3.9$ .<sup>16</sup>

#### IV. CONCLUSION

In summary, we investigated the spectral properties of the correlated  $3d^1$  systems SrVO<sub>3</sub> and CaVO<sub>3</sub> within the LDA+DMFT(QMC) approach. Constrained LDA was used to determine the average Coulomb interaction as  $\bar{U}=3.55$  eV and the exchange coupling as  $J=1.0$  eV. With this input we calculated the spectra of the two systems in a parameter-free way. Both systems are found to be strongly correlated metals, with a transfer of the majority of the spectral weight from the quasiparticle peak to the incoherent upper and lower Hubbard bands. Although the calculated DMFT spectra of SrVO<sub>3</sub> and CaVO<sub>3</sub> are slightly different above the Fermi energy, they are very similar, in particular, the quasiparticle part below the Fermi energy. Our calculated spectra agree very well with recent bulk-sensitive high-resolution PES (Ref. 18) and XAS,<sup>21</sup> i.e., with the experimental spectrum below and above the Fermi energy. Both compounds are similarly strongly correlated metals; CaVO<sub>3</sub> is not on the verge of a Mott-Hubbard transition.

Our results are in striking contrast to previous theories and the widespread expectation that the strong lattice distortion leads to a strong narrowing of the CaVO<sub>3</sub> bandwidth and, hence, much stronger correlation effects in CaVO<sub>3</sub>. While the  $e_g$  bands indeed narrow considerably, the competition between decreasing  $d-p-d$  and increasing  $d-d$  hybridization leads to a rather insignificant narrowing of the  $t_{2g}$  bands at the Fermi energy. This explains why CaVO<sub>3</sub> and SrVO<sub>3</sub> are so similar. With our theoretical results confirming the new PES and XAS experiments, we conclude that the insulating-like behavior observed in earlier PES and BIS experiments on CaVO<sub>3</sub> must be attributed to surface effects.<sup>20</sup>

#### ACKNOWLEDGMENTS

This work was supported by Russian Basic Research Foundation Grants No. 03-02-39024 (V.A., I.N., D.K.), 04-02-16096 (V.A., I.N., D.K.), 05-02-17244 (I.N.), 05-02-16301 (I.N.), and the Deutsche Forschungsgemeinschaft through Sonderforschungsbereich 484 (D.V., G.K., I.N.), and in part by the joint UrO-SO project N22 (V.A., I.N.), the Emmy-Noether program (KH). I.N. acknowledges support from programs of the Presidium of the Russian Academy of Sciences (RAS) "Quantum macrophysics" and of the Division of Physical Sciences of the RAS "Strongly correlated electrons in semiconductors, metals, superconductors and magnetic materials," a Grant of the President of the Russian Federation for Young Scientists MK-2118.2005.02, the Dynasty Foundation and International Center for Fundamental Physics in Moscow Program for Young Scientists 2005, and the Russian Science Support Foundation Program for Young Ph.D. of the Russian Academy of Sciences 2005.

- <sup>1</sup>R. O. Jones and O. Gunnarsson, *Rev. Mod. Phys.* **61**, 689 (1989).
- <sup>2</sup>J. Hubbard, *Proc. R. Soc. London, Ser. A* **276**, 238 (1963); **277**, 237 (1963); **281**, 401 (1964).
- <sup>3</sup>V. I. Anisimov, J. Zaanen, and O. K. Andersen, *Phys. Rev. B* **44**, 943 (1991); V. I. Anisimov, F. Aryasetiawan, and A. I. Lichtenstein, *J. Phys.: Condens. Matter* **9**, 767 (1997).
- <sup>4</sup>W. Metzner and D. Vollhardt, *Phys. Rev. Lett.* **62**, 324 (1989).
- <sup>5</sup>D. Vollhardt, in *Correlated Electron Systems*, edited by V. J. Emery (World Scientific, Singapore, 1993), p. 57.
- <sup>6</sup>Th. Pruschke, M. Jarrell, and J. K. Freericks, *Adv. Phys.* **44**, 187 (1995).
- <sup>7</sup>A. Georges, G. Kotliar, W. Krauth, and M. J. Rozenberg, *Rev. Mod. Phys.* **68**, 13 (1996).
- <sup>8</sup>G. Kotliar and D. Vollhardt, *Phys. Today* **57**(3), 53 (2004).
- <sup>9</sup>V. I. Anisimov, A. I. Poteryaev, M. A. Korotin, A. O. Anokhin, and G. Kotliar, *J. Phys.: Condens. Matter* **9**, 7359 (1997). The same strategy was formulated by Lichtenstein and Katsnelson, *Phys. Rev. B* **57**, 6884 (1998), as one of their LDA++ approaches.
- <sup>10</sup>K. Held, I. A. Nekrasov, G. Keller, V. Eyert, N. Blümer, A. K. Mc Mahan, R. T. Scalettar, Th. Pruschke, V. I. Anisimov, and D. Vollhardt, *Psi-k Newsletter* **56**, 65 (2003) [[psi-k.dl.ac.uk/newsletters/News\\_56/Highlight\\_56.pdf](http://psi-k.dl.ac.uk/newsletters/News_56/Highlight_56.pdf)].
- <sup>11</sup>A. I. Lichtenstein, M. I. Katsnelson, and G. Kotliar, in *Electron Correlations and Materials Properties*, edited by A. Gonis, N. Kioussis, and M. Cifan (Kluwer Academic/Plenum, New York, 2002), p. 428 [available as cond-mat/0112430].
- <sup>12</sup>A. Fujimori, I. Hase, H. Namatame, Y. Fujishima, Y. Tokura, H. Eisaki, S. Uchida, K. Takegahara, and F. M. F. de Groot, *Phys. Rev. Lett.* **69**, 1796 (1992).
- <sup>13</sup>Y. Aiura, F. Iga, Y. Nishihara, H. Ohnuki, and H. Kato, *Phys. Rev. B* **47**, 6732 (1993); I. H. Inoue, I. Hase, Y. Aiura, A. Fujimori, Y. Haruyama, T. Maruyama, and Y. Nishihara, *Phys. Rev. Lett.* **74**, 2539 (1995); I. H. Inoue, O. Goto, H. Makino, N. E. Hussey, and M. Ishikawa, *Phys. Rev. B* **58**, 4372 (1998).
- <sup>14</sup>K. Morikawa, T. Mizokawa, K. Kobayashi, A. Fujimori, H. Eisaki, S. Uchida, F. Iga, and Y. Nishihara, *Phys. Rev. B* **52**, 13711 (1995).
- <sup>15</sup>M. J. Rozenberg, I. H. Inoue, H. Makino, F. Iga, and Y. Nishihara, *Phys. Rev. Lett.* **76**, 4781 (1996).
- <sup>16</sup>H. Makino, I. H. Inoue, M. J. Rozenberg, I. Hase, Y. Aiura, and S. Onari, *Phys. Rev. B* **58**, 4384 (1998).
- <sup>17</sup>K. Maiti, D. D. Sarma, M. J. Rozenberg, I. H. Inoue, H. Makino, O. Goto, M. Pedio, and R. Cimino, *Europhys. Lett.* **55**, 246 (2001).
- <sup>18</sup>A. Sekiyama, H. Fujiwara, S. Imada, H. Eisaki, S. I. Uchida, K. Takegahara, H. Harima, Y. Saitoh, and S. Suga, cond-mat/0206471 (unpublished), superseded by Ref. 19.
- <sup>19</sup>A. Sekiyama, H. Fujiwara, S. Imada, S. Suga, H. Eisaki, S. I. Uchida, K. Takegahara, H. Harima, Y. Saitoh, I. A. Nekrasov, G. Keller, D. E. Kondakov, A. V. Kozhevnikov, Th. Pruschke, K. Held, D. Vollhardt, and V. I. Anisimov, *Phys. Rev. Lett.* **93**, 156402 (2004).
- <sup>20</sup>A. Liebsch, *Phys. Rev. Lett.* **90**, 096401 (2003).
- <sup>21</sup>I. H. Inoue, I. Hase, Y. Aiura, A. Fujimori, K. Morikawa, T. Mizokawa, Y. Haruyama, T. Maruyama, and Y. Nishihara, *Physica C* **235–240**, 1007 (1994).
- <sup>22</sup>I. A. Nekrasov, G. Keller, D. E. Kondakov, A. V. Kozhevnikov, Th. Pruschke, K. Held, D. Vollhardt, and V. I. Anisimov, cond-mat/0211508.
- <sup>23</sup>E. Pavarini, S. Biermann, A. Poteryaev, A. I. Lichtenstein, A. Georges, and O. K. Andersen, *Phys. Rev. Lett.* **92**, 176403 (2004).
- <sup>24</sup>During the publication of this paper the work by E. Pavarini, A. Yamasaki, J. Nuss, and O. K. Andersen, *New J. Phys.* **7**, 198 (2005), became available.
- <sup>25</sup>V. I. Anisimov, D. E. Kondakov, A. V. Kozhevnikov, I. A. Nekrasov, Z. V. Pchelkina, J. W. Allen, S.-K. Mo, H.-D. Kim, P. Metcalf, S. Suga, A. Sekiyama, G. Keller, I. Leonov, X. Ren, and D. Vollhardt, *Phys. Rev. B* **71**, 125119 (2005).
- <sup>26</sup>O. K. Andersen and T. Saha-Dasgupta, *Phys. Rev. B* **62**, R16219 (2000); O. K. Andersen, T. Saha-Dasgupta, S. Ezhov, L. Tssets-eris, O. Jepsen, R. W. Tank, C. Arcangeli, and G. Krier, *Psi-k Newsletter* **45**, 86 (2001); O. K. Andersen, T. Saha-Dasgupta, and S. Ezhov, *Bull. Mater. Sci.* **26**, 19 (2003).
- <sup>27</sup>I. A. Nekrasov, K. Held, G. Keller, D. E. Kondakov, Th. Pruschke, O. K. Andersen, V. I. Anisimov, D. Vollhardt, cond-mat/0508313 (unpublished).
- <sup>28</sup>I. H. Inoue (private communication).
- <sup>29</sup>M. J. Rey, P. H. Dehault, J. C. Joubert, B. Lambert-Andron, M. Cyrot, and F. Cyrot-Lackmann, *J. Solid State Chem.* **86**, 101 (1990).
- <sup>30</sup>B. L. Chamberland and P. S. Danielson, *J. Solid State Chem.* **3**, 243 (1971).
- <sup>31</sup>O. K. Andersen, *Phys. Rev. B* **12**, 3060 (1975); O. Gunnarsson, O. Jepsen, and O. K. Andersen, *Phys. Rev. B* **27**, 7144 (1983).
- <sup>32</sup>Logarithmic derivatives were fixed to the value  $-l-1$  for Sr( $p, f$ ), Ca( $p$ ), V( $d$ ), and O( $s, d$ ) states.
- <sup>33</sup>K. Takegahara, *J. Electron Spectrosc. Relat. Phenom.* **66**, 303 (1995).
- <sup>34</sup>O. Gunnarsson, O. K. Andersen, O. Jepsen, and J. Zaanen, *Phys. Rev. B* **39**, 1708 (1989).
- <sup>35</sup>I. Solovyev, N. Hamada, and K. Terakura, *Phys. Rev. B* **53**, 7158 (1996).
- <sup>36</sup>M. B. Zöfl, Th. Pruschke, J. Keller, A. I. Poteryaev, I. A. Nekrasov, and V. I. Anisimov, *Phys. Rev. B* **61**, 12810 (2000).
- <sup>37</sup>J. E. Hirsch and R. M. Fye, *Phys. Rev. Lett.* **56**, 2521 (1986). For multi-band QMC within DMFT see Ref. 10.
- <sup>38</sup>For a review on the maximum entropy method, see M. Jarrell and J. E. Gubernatis, *Phys. Rep.* **269**, 133 (1996).
- <sup>39</sup>A. Liebsch and A. Lichtenstein, *Phys. Rev. Lett.* **84**, 1591 (2000).
- <sup>40</sup>I. A. Nekrasov, K. Held, N. Blümer, A. I. Poteryaev, V. I. Anisimov, and D. Vollhardt, *Eur. Phys. J. B* **18**, 55 (2000).
- <sup>41</sup>K. Held, G. Keller, V. Eyert, D. Vollhardt, and V. I. Anisimov, *Phys. Rev. Lett.* **86**, 5345 (2001).
- <sup>42</sup>I. A. Nekrasov, Z. V. Pchelkina, G. Keller, Th. Pruschke, K. Held, A. Krimmel, D. Vollhardt, and V. I. Anisimov, *Phys. Rev. B* **67**, 085111 (2003).
- <sup>43</sup>Ph. Lambin and J. P. Vigneron, *Phys. Rev. B* **29**, 3430 (1984).
- <sup>44</sup>M. O. Krause and J. H. Oliver, *J. Phys. Chem. Ref. Data* **8**, 329 (1979).
- <sup>45</sup>I. H. Inoue, C. Bergemann, I. Hase, and S. R. Julian, *Phys. Rev. Lett.* **88**, 236403 (2002).